Molecular Pharmacology Fast Forward. Published on February 10, 2017 as DOI: 10.1124/mol.116.106013
This article has not been copyedited and formatted. The final version may differ from this version.

MOL #106013

Title: Differential effects of oxytocin receptor antagonists, Atosiban and Nolasiban, on OT-mediated signalling in human amnion and myometrium

Authors:
Sung Hye Kim, Oliver Pohl, Andre Chollet, Jean-Pierre Gotteland, Adam D.J. Fairhurst, Phillip R. Bennett and Vasso Terzidou.

Institute of Reproductive and Developmental Biology (IRDB), Imperial College London, Hammersmith Hospital Campus, Du Cane Road, London, W12 0NN, UK
- SK, ADJF, PRB, VT

ObsEva SA, Chemin des Aulx 12, CH-1228 Plan-les-Ouates, Geneva, Switzerland
- OP, AC, JPG

Imperial College School of Medicine, Chelsea and Westminster Hospital, 369 Fulham Road, London, SW10 9NH, UK
- VT

Downloaded from molpharm.aspetjournals.org at ASPET Journals on April 10, 2024

Molecular Pharmacology Fast Forward. Published on February 10, 2017 as DOI: 10.1124/mol.116.106013
This article has not been copyedited and formatted. The final version may differ from this version.

MOL #106013

Running title: Nolasiban suppresses OT-mediated inflammatory responses

Corresponding author: Dr. Vasso Terzidou, Tel: +44(0)20759 43720, Fax: +44(0)20 759 42148, Email: v.terzidou@imperial.ac.uk

Number of Text pages: 25

Number of Tables: 1

Number of Figures: 14 (plus two supplementary figures)

Number of References: 24

Number of words in Abstract: 239

Number of words in Introduction: 722

Number of words in Discussion: 884

List of Abbreviations:

Arginine vasopressin, AVP; G protein-coupled receptor, GPCR; inositol phosphate, IP_3; mitogen activated protein kinases, MAPKs; oxytocin, OT; oxytocin receptor, OTR; phospholipase A, PLA; phospholipase C, PLC; preterm labour, PTL; prostaglandin, PG; Proton nuclear magnetic resonance spectroscopy, ^1H NMR; superoxide dismutase 2, SOD2; Thin layer chromatography, TLC.

Downloaded from molpharm.aspetjournals.org at ASPET Journals on April 10, 2024

Molecular Pharmacology Fast Forward. Published on February 10, 2017 as DOI: 10.1124/mol.116.106013
This article has not been copyedited and formatted. The final version may differ from this version.

Abstract:

One of the most established roles of oxytocin (OT) is in inducing uterine contractions and labour. Apart from contractions, our recent study have shown that OT can also activate pro-inflammatory pathways in both human myometrial and amnion cells which suggests the pro-inflammatory role of OT should be taken into account when developing tocolytics targeting the OT/OT receptor (OT/OTR) system. The OTR antagonist, Atosiban, is currently used therapeutically for the treatment of PTL. We have previously shown that Atosiban fails to inhibit the pro-inflammatory effects of OT in human amnion, and Atosiban alone activates NF-κB and MAPKs thus upregulating downstream pro-labour genes. In contrast to our findings with Atosiban, the presence of the orally active OTR antagonist, Nolasiban, reduced the effect of OT on NF-κB and p38 kinase activation both in myometrial and amnion cells. Consistent with the activation of these inflammatory mediators, OT led to increases in the expression of COX-2 and p-cPLA$_2$, which was reflected in PGE$_2$ synthesis. Inhibition of NF-κB activation by Nolasiban also translated to suppression of downstream pro-labour gene expression such as COX-2, CCL2, IL-6, and IL-8. We have also demonstrated that Nolasiban treatment alone has no significant stimulatory effect on both the myometrium and amnion. In conclusion, our findings indicate that Nolasiban possesses a promising potential as a novel tocolytic agent for both acute and maintenance therapy as it inhibits both myometrial contractions and the pro-inflammatory effects of OT without the biased agonist effects.

Downloaded from molpharm.aspetjournals.org at ASPET Journals on April 10, 2024

Molecular Pharmacology Fast Forward. Published on February 10, 2017 as DOI: 10.1124/mol.116.106013
This article has not been copyedited and formatted. The final version may differ from this version.

Introduction:

Complications arising from preterm labour (PTL) account for 65% of neonatal deaths and 50% of neurological disabilities worldwide. Advances in the care of preterm infants have dramatically increased rates of survival, which rise sharply from 1% at 23 weeks to 99% at 32 weeks. However, this is associated with a reciprocal increase in the risk of handicap (Lawn *et al*, 2013). Although advances have been made in prediction and prevention of preterm birth in women identified at high risk based upon past history, the overall rate has not reduced. The 2012 WHO report "Born Too Soon" (Howson *et al*, 2013) highlighted the need for effective tocolytic drugs to delay preterm birth in women with preterm contractions.

Infection and/or inflammation is associated with activation of contractile pathways leading to both term and preterm labour. Furthermore, infection/inflammation and the subsequent increases in pro-inflammatory cytokines have been found to be one of the most potent causes of perinatal brain injury (Dommergues *et al*, 2000; Thornton *et al*, 2012). In normal birth weight infants at term, chorioamnionitis and intrauterine exposure to maternal infection are associated with periventricular leukomalacia and cerebral palsy (Grether & Nelson, 1997; Wu & Colford, 2000). In the case of established chorioamnionitis, it is possible that an effective tocolytic drug based solely on the inhibition of uterine contractions could result in prolonged exposure of fetus to an adverse environment. Therefore, an optimal tocolytic should also have an anti-inflammatory activity. While the precise mechanisms responsible for initiating labour in humans remain ambiguous, it is well established that the oxytocin/oxytocin receptor (OT/OTR) system plays a central role in the biochemistry of term/preterm labour. Functional OTR is expressed both in myometrium and fetal membranes (amnion and chorion). OT is widely used for induction/augmentation of both preterm and term labour, and OT binding to its receptor leads to OTR coupling with both $G_{\alpha q/11}$ and $G_{\alpha i/o}$ G-proteins (Phaneuf *et al*, 1993). $G_{\alpha q/11}$ signalling in myometrium activates phospholipase C (PLC) to drive increases in intracellular Ca^{2+} via inositol triphosphate (IP_3), ultimately leading to contractions. Previous studies have shown that OTR signalling through $G_{\alpha i/o}$ reduces cAMP by inhibition of adenylate cyclase activity (Blanks & Thornton, 2003; Busnelli *et al*, 2012). We have recently demonstrated a novel mechanism for OT driving pro-

Downloaded from molpharm.aspetjournals.org at ASPET Journals on April 10, 2024

Molecular Pharmacology Fast Forward. Published on February 10, 2017 as DOI: 10.1124/mol.116.106013
This article has not been copyedited and formatted. The final version may differ from this version.

inflammatory effects in human gestational tissues (Kim *et al*, 2015). In amnion, this was found to be via $G_{\alpha i}$ signalling, which leads to activation of mitogen activated protein kinases (MAPKs) and NF-κB, and subsequent increase in the expression of NF-κB regulated genes including prostaglandin synthetic enzymes and inflammatory chemokines/cytokines.

OTR antagonists are used in clinical practice for the treatment of preterm labour through inhibition of myometrial contractility, but their effect on the pro-inflammatory effects of OT has been largely ignored. We have recently shown that this OT-driven pro-inflammatory effects in amnion are not inhibited by Atosiban. Conversely, Atosiban alone results in activation of MAPKs and NF-κB to the same extent as OT (Kim *et al*, 2016). Atosiban acts as a biased ligand to the $G_{\alpha i}$ pathway which may limit its use to 48 hours (Busnelli *et al*, 2012; Haas *et al*, 2012), yet OTR still represents an attractive drug target for tocolysis. Indeed, with growing recognition of the complexity of G protein-coupled receptor (GPCR) signalling, there has been an impetus to design more specific compounds modulating GPCR action that show bias towards specific signalling pathways (Busnelli *et al*, 2012; Whalen *et al*, 2011).

All clinical studies to date have used OTR antagonists for acute tocolysis rather than for the prevention of PTL in women at high risk for preterm delivery. The only OTR antagonist currently licensed in Europe is Atosiban which can only be given as a continuous IV infusion for no more than 48 hours thus precluding long-term administration for maintenance therapy. Nolasiban is a novel small molecule, non-peptide OTR antagonist. Nolasiban is selective for OTR against the arginine vasopressin (AVP) V1a and V2 receptors, whereas Atosiban is primarily a V1a antagonist (Manning *et al*, 2001). While the currently available OTR antagonist Atosiban is given via intravenous infusion, Nolasiban is administered orally thus lending itself to preterm labour treatment beyond 48 hours.

In this study we have investigated whether the OTR antagonist, Nolasiban, can inhibit the OT-driven activation of inflammatory response in human gestational tissues and we have compared and contrasted its effects with the currently licensed OTR antagonist Atosiban.

Downloaded from molpharm.aspetjournals.org at ASPET Journals on April 10, 2024

Molecular Pharmacology Fast Forward. Published on February 10, 2017 as DOI: 10.1124/mol.116.106013
This article has not been copyedited and formatted. The final version may differ from this version.

Materials and Methods:

Cell culture

Placentas with fetal membranes and myometrial biopsies were collected from term (38+0 - 40 weeks of pregnancy), non-labouring women with singleton pregnancies undergoing scheduled low-risk elective caesarean section. Those with pre-existing medical conditions, pre-eclampsia, multiple pregnancies and/or had received uterotonics prior to their caesarean sections were excluded from the study. Samples were collected following an informed consent and with approval from the local research ethics committees for Queen Charlotte's and Chelsea Hospital (Placenta; RREC 2002-6283 and Myometrium; RREC 1997-5089).

From the placenta, the amnion layer was pulled apart from the chorion to use for culture. Primary amnion epithelial cells were established from fetal membranes as previously described (Bennett *et al*, 1987). For myometrial smooth muscle cell isolation, the biopsies were dissected into fine pieces and digested in filter-sterilised collagenase mix (1mg/ml collagenase 1A, 1mg/ml collagenase X and 2mg/ml BSA in 1:1 ratio of DMEM/Nutrient Mixture F-12 HAM and serum-free DMEM, Sigma-Aldrich) for 45 min at 37°C. The digestion process was halted using DMEM with 10% v/v fetal calf serum (FCS) and the cell suspension was obtained by filtering out the tissue through a 40µm cell strainer (Corning). Centrifugation of the suspension at 3000rpm for 5 min collected the cells into a pellet, which was subsequently resuspended in full DMEM (10% FCS, 2mM LG, and 100U/ml PS) and cultured in cell culture-treated flasks (Corning) at 37°C in humidified atmosphere of 95% air and 5% CO_2. When myometrial cells reached 95% confluence, they were passaged using 0.25% trypsin with 0.02% EDTA in PBS. We used myometrial cells between passage numbers one to four.

Real time RT-PCR

Extraction of total RNA was carried out using RNA STAT-60 reagent for a guanidiumthiocyanate-phenol-chloroform extraction (AMS Biotechnology), following recommended manufacturer's protocol.

Downloaded from molpharm.aspetjournals.org at ASPET Journals on April 10, 2024

Molecular Pharmacology Fast Forward. Published on February 10, 2017 as DOI: 10.1124/mol.116.106013
This article has not been copyedited and formatted. The final version may differ from this version.

Any potential DNA contaminations were eliminated from the extracted RNA by DNaseI treatment (Invitrogen) prior to cDNA synthesis. The DNaseI-treated RNA was used for first-strand cDNA synthesis by M-MLV reverse transcriptase (Sigma-Aldrich). The changes in gene expression were determined by real-time PCR (RT-PCR) with ABI StepOne Plus Real Time PCR system (Applied Biosystems) using SYBR Green JumpStart *Taq* ReadyMix (Sigma-Aldrich). Primer Express (Applied Biosystems) software was used to design specific primers for each gene. The sequences of the gene specific primers are listed in Table 1. The resulting data were analysed using StepOne Software Version2.3 (Applied Biosystems). All primers were tested for efficiency and comparative Ct method was used to analyse the relative changes in the gene expression. Ct values for all target gene were normalised to L-19, the constitutively expressed ribosomal protein and also to GAPDH for amnion and myometrial cells, respectively.

Western Blotting

Whole-cell lysates were obtained by lysing the monolayer of cells in modified radioimmunoprecipitation assay (RIPA) buffer (150mM NaCl, 10mM Tris (pH 7.4), 1% Triton X-100, 0.1% SDS, 1% Sodium Deoxycholate, 1mM EDTA, 1mM PMSF, and protease and phosphotase inhibitor cocktails; Sigma-Aldrich, Thermo-fisher). Concentration of each lysate was determined using DC™ (detergent compatible) protein assay kit (Bio-Rad) and 40µg of each protein sample was denatured in loading dye with 50mM DTT by heating for 10 min at 80°C. Proteins were separated by electrophoresis on a 10% SDS-polyacrylamide gel for 80 min at constant 140V and transferred to PVDF membrane (Millipore) in wet-transfer chamber system (Bio-Rad) for 90 min at constant 300mA. For separating more than 15 protein samples, a pre-cast midi-gel (Bio-Rad) was used. The PVDF membranes were blocked in blocking buffer (5% w/v milk powder in TBS with 0.1% Tween-20) prior to the primary antibody incubation overnight at 4°C. HRP-conjugated secondary antibody incubation lasted for 1-2h at room temperature and signal detection was carried out using ECL reagent (Bio-Rad).

Downloaded from molpharm.aspetjournals.org at ASPET Journals on April 10, 2024

Molecular Pharmacology Fast Forward. Published on February 10, 2017 as DOI: 10.1124/mol.116.106013
This article has not been copyedited and formatted. The final version may differ from this version.

To confirm equal loading of samples, the membranes were treated with a mild stripping buffer (0.2M NaOH) and re-probed for β-actin.

Enzyme-linked immunosorbent assay (ELISA)

Concentrations of PGE_2 in the culture supernatants were determined by a standard ELISA. At completion of treatments, the culture media from both myometrial and amnion cells were collected and immediately frozen for storage at -20°C until subsequent analysis by ELISA, following the manufacturer's instructions (R&D systems).

Materials

The goat anti-COX-2 (C20) antibody (Santa Cruz Biotechnologies) was used at 1:2000 dilution and rabbit monoclonal antibodies to p-$cPLA_2$; p-p65 (Ser536); p-MAPK14 (p38 MAPK) and p-MAPK3/1 (ERK1/2 p44/42 MAPK) from Cell Signalling Technology were used at 1:1000 dilution. The mouse monoclonal anti-β-actin antibody (at 1:50,000) was from Abcam. HRP-conjugated secondary antibodies against goat, mouse and rabbit IgGs were from Santa Cruz Biotechnologies. Oxytocin and Atosiban were obtained from Alliance Pharmaceuticals and Sigma-Aldrich, respectively. Nolasiban was synthesised as previously described (Chollet, 2015). Nolasiban chemical formula is (3Z,5S)-5-(hydroxymethyl)-1-[(2′-methyl-1,1′-biphenyl-4-yl)carbonyl]pyrrolidin-3-one O-methyloxime (Fig 1). Nolasiban is prepared following an 8-step synthesis starting from 4-bromobenzoic acid. A detailed description of Nolasiban preparation is provided below;

A solution of potassium carbonate in water was charged to a slurry of 4-bromobenzoic acid in water at 15 to 25°C. The resulting slurry was stirred at 15 to 25°C and degassed three times using a vacuum-nitrogen purge cycle. Tetrakis (triphenylphosphine) palladium (0) was charged and the vacuum-nitrogen purge cycle repeated. A solution of o-tolylboronic acid was degassed three times, using a vacuum-nitrogen purge cycle, and then charged to the 4-bromobenzoic acid slurry at 15 to 25°C. The

Downloaded from molpharm.aspetjournals.org at ASPET Journals on April 10, 2024

Molecular Pharmacology Fast Forward. Published on February 10, 2017 as DOI: 10.1124/mol.116.106013
This article has not been copyedited and formatted. The final version may differ from this version.

reaction mixture was heated to and maintained at reflux until reaction completion (The reaction is considered complete at 95% conversion), as determined by ^{1}H NMR analysis (d6-DMSO), typically 1.5 to 2.5 hours. After work-up, the solid was dried in a vacuum oven at 35 to 40°C to give 4-(2-methylphenyl)benzoic acid ^{1}H NMR (d6-DMSO) concordant with structure] as a pale yellow solid. Thionyl chloride was added to a slurry of 4-(2-methylphenyl)benzoic acid in toluene at 10 to 25°C and the mixture was heated to and maintained at 75 to 80°C until complete by ^{1}H NMR analysis (d6-benzene), typically 4 to 5 hours. After work-up, the toluene solution of 4-(2-methylphenyl)benzoic acid chloride [^{1}H NMR (d6-benzene) concordant with structure] was used directly in the next step.

A solution of potassium carbonate was charged to a solution of 4-hydroxy-L- in tetrahydrofuran and water at 15 to 25°C followed by a line rinse of water. The mixture was cooled to 0 to 5°C with rapid stirring and a solution of 4-(2-methylphenyl)benzoic acid chloride in toluene charged at that temperature followed by a line rinse of toluene The reaction mixture was warmed to 15 to 25°C over 1 to 2 hours and stirred at this temperature until judged complete by TLC analysis. After work-up, the collected solid was dried under vacuum at 40 to 45°C until the water content by Karl Fischer titration was ≤0.2% w/w to afford (4R)-4-hydroxy-1-[(2'- methyl-1 ,1 '-biphenyl-4-yl)carbonyl]-L-proline [^{1}H NMR (d6-DMSO) concordant with structure] as an off-white solid.

Triethylamine was charged to a solution of (4R)-4-hydroxy-1-[(2'-methyl-1,1'-biphenyl-4-yl)carbonyl]-L-proline in DMSO at 15 to 20°C. Pyridine-sulphur trioxide complex was charged portion-wise at 15 and 25°C and the reaction mixture was stirred at that temperature until reaction completion, as determined by TLC analysis (typically 1 to 3 hours). After work-up, the collected solid was dried under vacuum at 40 to 45°C to give 1-[(2'-methyl-1,1'- biphenyl-4-yI)carbonyl]-4-oxo-L-proline [^{1}H NMR (d_6-DMSO) concordant with structure] as an off-white solid.

Triethylamine was added to a solution of 1-[(2'-methyl-1,1'-biphenyl-4-yl)carbonyl]-4-oxo-L-proline in dichloromethane at 10 to 25°C. Methoxylamine hydrochloride was added portionwise at 10 to 25°C and the reaction mixture was stirred at 10 to 25°C until reaction completion, as determined by TLC analysis (typically 3 to 5 hours, TLC eluent: dichloromethane:methanol:acetic acid (90:10:1); uv

Downloaded from molpharm.aspetjournals.org at ASPET Journals on April 10, 2024

Molecular Pharmacology Fast Forward. Published on February 10, 2017 as DOI: 10.1124/mol.116.106013
This article has not been copyedited and formatted. The final version may differ from this version.

visualization). After work-up, the filtrate and washes were combined and concentrated under vacuum at 35 to 40°C to afford 4-methoxyimino-1-[(2'-methyl-1,1'-biphenyl-4-yl)carbonyl]-L-proline [^{1}H NMR (CDCl3) concordant with structure) as an off-white solid.

Potassium carbonate was added to a solution of 4-methoxyimino-1-[(2'- methyl-1,1'-biphenyl-4-yl)carbonyl]-L-proline and the mixture cooled to 0 to 10°C. Dimethyl sulfate was added at 0 to 15°C and the mixture was stirred at 15 to 25°C until reaction completion, as determined by TLC analysis, typically 3 to 16 hours. After work-up, excess ethyl acetate was removed by azeotropic distillation with tetrahydrofuran under vacuum at 40 to 45°C to give (4Z/E, 2S)-methyl-1-[(2'-methyl-1,1'-biphenyl-4-yl)-carbonyl]-4- methoxyimino pyrrolidine-2-carboxylate [^{1}H NMR (CDCl3) concordant with structure] as a viscous brown oil.

Lithium borohydride was added portionwise under nitrogen to a stirred solution of (4Z/E, 2S)-methyl-1-[(2'-methyl-1,1'-biphenyl-4-yl)-carbonyl]-4- methoxyimino pyrrolidine-2-carboxylate in tetrahydrofuran and methanol at 0 to 30°C. The prepared mixture was stirred at 15 to 25°C to reaction completion, as determined by TLC analysis (Eluent: ethyl acetate; Visualisation: ninhydrin), typically 2 to 6 hours. After work-up, the combined filtrate and wash were concentrated under vacuum to give a crude isomeric mixture comprising (3Z,5S)-5-(hydroxymethyl)-1-[(2′-methyl-1,1′-biphenyl-4-yl)carbonyl]pyrrolidin-3-one O-methyloxime and (3E,5S)-5-(hydroxymethyl)-1-[(2′-methyl-1,1′-biphenyl-4-yl)carbonyl]pyrrolidin-3-one O-methyloxime [^{1}H NMR (CDCl3) concordant with structure; 82.0% area by HPLC, 71.4:28.6 Z/E ratio] as a viscous brown oil. The oil was dissolved in toluene and stored until required. Pure Nolasiban or (3Z,5S)-5-(hydroxymethyl)-1-[(2′-methyl-1,1′-biphenyl-4-yl)carbonyl]pyrrolidin-3-one O-methyloxime was isolated by chromatography and elution with Toluene:MeOH (99:1 v/v).

Vehicle for OT was DMEM (Sigma-Aldrich), Atosiban was dissolved in double deionized water, and Nolasiban in DMSO. Nolasiban was diluted from stock solutions using DMEM shortly prior to the treatments. The DMSO concentration was adjusted to 0.1% v/v in all dose formulations and control wells for Nolasiban experiments were treated to contain 0.1% v/v DMSO.

Downloaded from molpharm.aspetjournals.org at ASPET Journals on April 10, 2024

Molecular Pharmacology Fast Forward. Published on February 10, 2017 as DOI: 10.1124/mol.116.106013
This article has not been copyedited and formatted. The final version may differ from this version.

Statistical analysis

Prism software v5.0 (Graphpad) was used for our statistical analysis. We tested our data sets for normality using the *Kolmogorov-Smirnov* test prior to appropriate statistical comparisons. When data were normally distributed, multiple comparisons for all pairwise comparisons were performed using ANOVA, followed by *Tukey-Kramer* (or *Tukey's HSD*) *post hoc* test. For not-normally distributed data, multiple comparisons were performed using *Freidman's* test, followed by *Dunn's Multiple Comparisons post hoc* test. In this study, all data sets were presented as mean ± SEM values and the significant statistical differences with probability value of $p < 0.05$ are indicated with '*' in all figures.

Results:

Atosiban has no effect on OT-mediated upregulation of pro-inflammatory mediators, but mimics the effects of OT in human amnion

We have previously demonstrated that Atosiban presence in amnion cells has no significant effect on the OT-driven activation of NF-κB and MAPKs, and the upregulation of downstream pro-labour genes at OT concentration of 100nM (Kim *et al*, 2016). In this study, amnion cells were treated with Atosiban and a lower dose of OT (10nM), which is more physiologically relevant. There was no significant inhibition of OT effects in presence of Atosiban and similar to recently published data, Atosiban consistently led to activation of pro-inflammatory mediators including NF-κB and MAPKs and subsequent expression of prostaglandin (PG) synthetic enzymes COX-2 and p-cPLA$_2$ (Fig 2).

These effects of Atosiban translated to changes in the expression of downstream NF-κB regulated genes. The presence of Atosiban did not inhibit OT-mediated expression of COX-2, IL-6, CCL5, IL-8 and SOD2 at mRNA level (Fig 3). Furthermore, Atosiban treatment alone resulted in 2.8-, 2.3- and 2.4-fold increases in the expression of COX-2 ($p<0.05$), IL-6 ($p<0.05$) and CCL5 ($p<0.05$), respectively (Fig 3A-C).

Downloaded from molpharm.aspetjournals.org at ASPET Journals on April 10, 2024

Molecular Pharmacology Fast Forward. Published on February 10, 2017 as DOI: 10.1124/mol.116.106013
This article has not been copyedited and formatted. The final version may differ from this version.

Unlike Atosiban, Nolasiban suppresses the effects of OT on pro-inflammatory mediators including activation of NF-κB and MAPKs, and pro-labour gene expression in human amnion

Matching experiments in amnion cells using Nolasiban showed markedly different results to Atosiban. The presence of Nolasiban led to significant reduction in OT-driven activation of both NF-κB p65 and p38 kinase at equimolar concentration of Atosiban as well as at lower doses (Fig 4A-C). There was a slight reduction in OT-induced ERK1/2 activation in a dose dependent manner, however, this did not reach significance (Fig 4D). Nolasiban alone did not have a significant effect on NF-κB and p38 activation, or the expression of PG synthetic enzymes (Supplementary Fig S1). However, at the maximum dose of Nolasiban, 30 μM, we observed activation of ERK1/2 ($p<0.001$) with no effect on downstream targets, indicating that at this high concentration of Nolasiban which is physiologically irrelevant, the effect may be due to activation of an alternative signalling pathway, independent to that of OT.

Treatment of amnion cells with Nolasiban also completely inhibited OT-mediated expression of PG synthetic enzymes, COX-2 and p-cPLA$_2$, from the lowest dose of 1μM ($p<0.05$ and $p<0.001$, respectively, Fig 5) and consequently, OT-mediated PGE_2 release ($p<0.001$; Fig 6). Further experiments looking at the mRNA expression of other NF-κB regulated genes revealed a clear dose-dependent inhibitory effect of Nolasiban on COX-2, IL-6, CCL5, IL-8, CCL2 and SOD2 (Fig 7).

Atosiban acts as a partial inhibitor of OT-mediated responses, but it alone consistently activates NF-κB and ERK1/2, whilst inducing CCL5 expression in human myometrium

In contrast to our findings in human amnion, treatment with Atosiban significantly reduced OT-driven activation of p38 kinase and the upregulation of COX-2 in human myometrial cells (Fig 8). However, despite these inhibitory effects, Atosiban failed to suppress the effect of OT on NF-κB and ERK1/2 activation and on the reverse resulted in activation of both NF-κB and ERK1/2 in the absence of OT (Fig 8).

Presence of Atosiban showed variable effects on the expression of downstream NF-κB regulated genes. Complementary to the findings in COX-2 expression at protein level, Atosiban successfully inhibited

Downloaded from molpharm.aspetjournals.org at ASPET Journals on April 10, 2024

Molecular Pharmacology Fast Forward. Published on February 10, 2017 as DOI: 10.1124/mol.116.106013
This article has not been copyedited and formatted. The final version may differ from this version.

the OT-induced mRNA expression of COX-2 and IL-8 (Fig 9A and D). There was marginal reduction in OT-induced IL-6 expression, but not reaching statistical significance (Fig 9B). Of particular note were the changes in the mRNA expression of CCL5 which increased with Atosiban in the absence of OT stimulation (Fig 9C).

Similar to amnion, Nolasiban suppresses the effects of OT on pro-inflammatory mediators in human myometrium

Myometrial smooth muscle cells were incubated with increasing doses of Nolasiban with or without OT stimulation. The OTR antagonist, Nolasiban, alone had no significant effect on the OT-induced activation of NF-κB and MAPKs, and the presence of Nolasiban blocked the effects of OT on NF-κB and p38 kinase, reaching significance at the dose of 10μM (p<0.01; Fig 10). Moreover, Nolasiban suppressed the OT-driven upregulation of COX-2 and p-cPLA$_2$ (Fig 11), ultimately leading to the reduction of PGE$_2$ synthesis (Fig 12). In addition to COX-2 expression, Nolasiban also resulted in suppression of other NF-κB regulated genes, IL-8, IL-6, and CCL5, in a dose dependent manner (Fig 13 A-D). Similar to amnion, Nolasiban treatment alone in myometrium had no effect on the activation of NF-κB and p38, or the expression of PG synthetic enzymes (Supplementary Fig S2). Nolasiban at 30 μM activated of ERK1/2 (p<0.01) without affecting the expression of downstream targets such as COX-2 and p-cPLA$_2$.

Discussion:

We have investigated the effect of Nolasiban, a novel orally active OTR antagonist, on OT-driven activation of inflammatory responses in human gestational tissues. We have previously shown that OT activates a cassette of inflammatory mediators in both human amnion and myometrium, demonstrating a role for OT as an endogenous inflammatory signalling molecule (Kim *et al*, 2015). Atosiban, an OTR antagonist, is used in clinical practice in Europe for the treatment of preterm labour and other OTR antagonists are in clinical trials. Although OTR antagonists can inhibit myometrial contractility they appear to have differential effects upon mediators of inflammation within the gestational tissues. The

Downloaded from molpharm.aspetjournals.org at ASPET Journals on April 10, 2024

Molecular Pharmacology Fast Forward. Published on February 10, 2017 as DOI: 10.1124/mol.116.106013
This article has not been copyedited and formatted. The final version may differ from this version.

OTR antagonist Atosiban has been shown to inhibit myometrial contractility (Phaneuf *et al*, 1994), however, Atosiban only acts as a partial inhibitor of OT-mediated pro-inflammatory responses in human myometrium and has a purely stimulatory and no inhibitory effect in human amnion. We have shown that in contrast to Atosiban, Nolasiban suppresses OT-mediated pro-inflammatory effects in both human amnion and myometrium (Fig 14).

We have previously shown that there are differences in OT-mediated activation of NF-κB between amnion and myometrium which are associated with differential NF-κB subunit translocation and MAPKs crosstalk. In myometrium, OT-driven NF-κB activation resembles a canonical NF-κB signalling pathway involving both p65 and p50 translocation. OT-induced NF-κB activation in amnion involves nuclear translocation of p65 but not p50, and requires ERK1/2 and p38 activation (Kim *et al*, 2015). Such tissue-specific signalling may provide an explanation for the variable effects of Atosiban in amnion and myometrium where it acts as an 'anti-labour' agent though inhibition of OT-induced contractility in myometrium, whilst acting as a 'pro-labour agent' in amnion and partially so in myometrium possibly via differential OTR G-protein coupling in the two cell types. In amnion, Atosiban has no inhibitory effect and notably, it alone mimics the pro-inflammatory effects of OT whereas in myometrium, Atosiban significantly reduces OT-driven activation of p38 kinase and the upregulation of COX-2, and IL-8 but remains unable to suppress the effect of OT on NF-κB and ERK1/2 activation and increases CCL5 expression regardless of OT stimulation. The data which we present here shows that, unlike Atosiban, Nolasiban completely inhibits all OT-mediated responses and suppresses expression and activation of pro-inflammatory mediators both in amnion and myometrium without any downstream effects when treated alone. Despite the complete inhibition of OT-induced COX-2 upregulation and PGE_2 levels in presence of Nolasiban, relatively high levels of PGE_2 were detected in samples treated with Nolasiban and OT at earlier time points. This may be due to the release of PGE_2 rather than synthesis as Nolasiban successfully inhibits COX-2 expression as early as 2 h. There has been reports in rat models where OT was able to stimulate immediate pulsatile release of PGE_2 via Ca^{2+} responses (Chen *et al*, 2015).

Downloaded from molpharm.aspetjournals.org at ASPET Journals on April 10, 2024

Molecular Pharmacology Fast Forward. Published on February 10, 2017 as DOI: 10.1124/mol.116.106013
This article has not been copyedited and formatted. The final version may differ from this version.

Preterm and term labour are characterised by a marked inflammatory cascade (Osman *et al*, 2003; Shynlova *et al*, 2013) associated with the upregulation of pro-inflammatory cytokines and chemokines, such as IL-1β, IL-6, IL-8, CCL2 and CCL5, in both human amnion and myometrium. Amnion is an important site of prostaglandin and pro-inflammatory cytokine/chemokine release and leads to fetal membrane remodelling and cervical ripening (Kim *et al*, 2015). Fetal membrane activation is considered to be a prelude to the onset of labour (Lim *et al*, 2012). This involves activation of inducible NF-κB and the upregulation of pro-labour pro-inflammatory genes such as COX-2 and OTR (Lim *et al*, 2012). We have previously demonstrated that treatment with OT drives a similar set of inflammatory gene expression as those in amnion activation, indicating that OT may act as an endogenous inflammatory signalling molecule in human gestational tissues (Kim *et al*, 2015).

Knowledge of G protein-coupled receptors (GPCRs) continues to evolve, and the diversity of its actions and complexity of its signalling mechanisms are becoming increasingly evident (Berchiche & Sakmar, 2016). The biology of the OT/OTR system appears to be no exception. Nolasiban is a novel orally active, small molecule, non-peptide OTR antagonist which is more selective for OTR than Atosiban as it binds to the human OTR with a K_i of 52nM and is 2.5- and 50- fold selective against the AVP V1a and V2 receptors, respectively. We have previously shown that Nolasiban can inhibit spontaneous and OT-stimulated contractions in a dose-dependent way, affecting the rate, the contraction peak, the tension and the contraction duration to similar extent as Atosiban (Arulkumaran *et al*, 2016). Unlike Atosiban, inhibition of uterine contractions by Nolasiban did not evoke a proinflammatory signalling pathway, therefore, it appears to be a pure OTR antagonist, blocking both $G_{\alpha i}$ and $G_{\alpha q}$ mediated OT signalling in both amnion and myometrium.

Early preterm birth, typically classified as delivery before 34 weeks of gestation, is often associated with infection and/or inflammation. It is now recognized that cytokine-mediated cerebral injury represents an important cause of prematurity linked handicap, thus inflammation within the uterus is a important risk factor for fetal and neonatal CNS damage and poor outcome (Peebles, 2007). Therefore, it is crucial that any tocolytic agent used in acute preterm labour, including those modulating the OT/OTR system, should evade activation or aggravation of inflammation. The current study indicates

Downloaded from molpharm.aspetjournals.org at ASPET Journals on April 10, 2024

Molecular Pharmacology Fast Forward. Published on February 10, 2017 as DOI: 10.1124/mol.116.106013
This article has not been copyedited and formatted. The final version may differ from this version.

that Nolasiban is a promising new tocolytic as it has the ability not only to inhibit myometrial contractility but can also suppress the OT-mediated pro-inflammatory responses in human gestational tissues.

Acknowledgements:

The authors would like to thank labour ward patients and staff at Queen Charlotte's and Chelsea hospital, who provided and assisted the collection of placenta and myometrial biopsies.

Authorship contributions:

Participated in research design: Kim, Bennett and Terzidou

Conducted experiments: Kim and Fairhurst

Contributed new reagents or analytic tools: Pohl, Gotteland and Chollet

Performed data analysis: Kim, Bennett and Terzidou

Wrote or contributed to the writing of the manuscript: Kim, Pohl, Gotteland, Chollet, Bennett and Terzidou

Downloaded from molpharm.aspetjournals.org at ASPET Journals on April 10, 2024

Molecular Pharmacology Fast Forward. Published on February 10, 2017 as DOI: 10.1124/mol.116.106013
This article has not been copyedited and formatted. The final version may differ from this version.

References:

Arulkumaran S, Kim SH, Pohl O, Chollet A, Bennett PR, terzidou V (2016) The OTR antagonist, OBE001, inhibits both spontaneous and OT-induced contractions of human pregnant myometrium in vitro. *Reproductive sciences* **23**

Bennett PR, Rose MP, Myatt L, Elder MG (1987) Preterm labor: stimulation of arachidonic acid metabolism in human amnion cells by bacterial products. *Am J Obstet Gynecol* **156:** 649-655

Berchiche YA, Sakmar TP (2016) CXC Chemokine Receptor 3 Alternative Splice Variants Selectively Activate Different Signaling Pathways. *Mol Pharmacol*

Blanks AM, Thornton S (2003) The role of oxytocin in parturition. *BJOG : an international journal of obstetrics and gynaecology* **110 Suppl 20:** 46-51

Busnelli M, Sauliere A, Manning M, Bouvier M, Gales C, Chini B (2012) Functional selective oxytocin-derived agonists discriminate between individual G protein family subtypes. *J Biol Chem* **287:** 3617-3629

Chen D, Zhao J, Wang H, An N, Zhou Y, Fan J, Luo J, Su W, Liu C, Li J (2015) Oxytocin evokes a pulsatile PGE2 release from ileum mucosa and is required for repair of intestinal epithelium after injury. *Scientific reports* **5:** 11731

Chollet A. (2015) Pyrrolidine derivatives as oxytocin/vasopressin V1a receptors antagonists. In Organization WIP (ed.).

Dommergues MA, Patkai J, Renauld JC, Evrard P, Gressens P (2000) Proinflammatory cytokines and interleukin-9 exacerbate excitotoxic lesions of the newborn murine neopallium. *Ann Neurol* **47:** 54-63

Grether JK, Nelson KB (1997) Maternal infection and cerebral palsy in infants of normal birth weight. *JAMA : the journal of the American Medical Association* **278:** 207-211

Haas DM, Caldwell DM, Kirkpatrick P, McIntosh JJ, Welton NJ (2012) Tocolytic therapy for preterm delivery: systematic review and network meta-analysis. *Bmj* **345:** e6226

Howson CP, Kinney MV, McDougall L, Lawn JE, Born Too Soon Preterm Birth Action G (2013) Born too soon: preterm birth matters. *Reproductive health* **10 Suppl 1:** S1

Kim SH, MacIntyre DA, Firmino Da Silva M, Blanks AM, Lee YS, Thornton S, Bennett PR, Terzidou V (2015) Oxytocin activates NF-kappaB-mediated inflammatory pathways in human gestational tissues. *Molecular and cellular endocrinology* **403:** 64-77

Downloaded from molpharm.aspetjournals.org at ASPET Journals on April 10, 2024

Molecular Pharmacology Fast Forward. Published on February 10, 2017 as DOI: 10.1124/mol.116.106013
This article has not been copyedited and formatted. The final version may differ from this version.

Kim SH, MacIntyre DA, Hanyaloglu AC, Blanks AM, Thornton S, Bennett PR, Terzidou V (2016) The oxytocin receptor antagonist, Atosiban, activates pro-inflammatory pathways in human amnion via Galphai signalling. *Molecular and cellular endocrinology* **420:** 11-23

Lawn JE, Davidge R, Paul VK, von Xylander S, de Graft Johnson J, Costello A, Kinney MV, Segre J, Molyneux L (2013) Born too soon: care for the preterm baby. *Reproductive health* **10 Suppl 1:** S5

Lim S, Macintyre DA, Lee YS, Khanjani S, Terzidou V, Teoh TG, Bennett PR (2012) Nuclear factor kappa B activation occurs in the amnion prior to labour onset and modulates the expression of numerous labour associated genes. *PLoS One* **7:** e34707

Manning M, Stoev S, Cheng LL, Wo NC, Chan WY (2001) Design of oxytocin antagonists, which are more selective than atosiban. *Journal of peptide science : an official publication of the European Peptide Society* **7:** 449-465

Osman I, Young A, Ledingham MA, Thomson AJ, Jordan F, Greer IA, Norman JE (2003) Leukocyte density and pro-inflammatory cytokine expression in human fetal membranes, decidua, cervix and myometrium before and during labour at term. *Molecular Human Reproduction* **9:** 41-45

Peebles DM. (2007) Intrauterine infection and perinatal brain injury. *Scientific Advisory Committee Opinion Paper 3 RCOG.*

Phaneuf S, Asboth G, MacKenzie IZ, Melin P, Lopez Bernal A (1994) Effect of oxytocin antagonists on the activation of human myometrium in vitro: atosiban prevents oxytocin-induced desensitization. *Am J Obstet Gynecol* **171:** 1627-1634

Phaneuf S, Europe-Finner GN, Varney M, MacKenzie IZ, Watson SP, Lopez Bernal A (1993) Oxytocin-stimulated phosphoinositide hydrolysis in human myometrial cells: involvement of pertussis toxin-sensitive and -insensitive G-proteins. *J Endocrinol* **136:** 497-509

Shynlova O, Lee YH, Srikhajon K, Lye SJ (2013) Physiologic uterine inflammation and labor onset: integration of endocrine and mechanical signals. *Reproductive sciences* **20:** 154-167

Thornton C, Rousset CI, Kichev A, Miyakuni Y, Vontell R, Baburamani AA, Fleiss B, Gressens P, Hagberg H (2012) Molecular mechanisms of neonatal brain injury. *Neurol Res Int* **2012:** 506320

Whalen E, Rajagopal S, Lefkowitz R (2011) Therapeutic potential of β-arrestin- and G protein-biased agonists. *Trends in molecular medicine* **17:** 126-165

Wu YW, Colford JM, Jr. (2000) Chorioamnionitis as a risk factor for cerebral palsy: A meta-analysis. *JAMA : the journal of the American Medical Association* **284:** 1417-1424

Downloaded from molpharm.aspetjournals.org at ASPET Journals on April 10, 2024

Molecular Pharmacology Fast Forward. Published on February 10, 2017 as DOI: 10.1124/mol.116.106013
This article has not been copyedited and formatted. The final version may differ from this version.

Footnotes:

This work was supported in part by Genesis Research Trust (Grant ref. P14758) and the National Institute for Health Research (NIHR) Biomedical Research Centre based at Imperial College Healthcare NHS Trust (Grant ref. P45272) and Imperial College London.

Disclosure Statement:

VT has worked as a consultant to GlaxoSmithKline. PB has worked as a consultant to Boehringer Ingelheim, GlaxoSmithKline, Merck Serono, ObsEva SA and Tokyo Tanabe Pharmaceuticals, drug companies with an interest in the pharmacological effects of oxytocin and oxytocin antagonists. PB holds shares of ObsEva SA. AC, JPG and OP are salaried employees of ObsEva SA.

Downloaded from molpharm.aspetjournals.org at ASPET Journals on April 10, 2024

Molecular Pharmacology Fast Forward. Published on February 10, 2017 as DOI: 10.1124/mol.116.106013
This article has not been copyedited and formatted. The final version may differ from this version.

Figure legends:

Figure 1. Chemical structure of Nolasiban.

Figure 2. The effect of Atosiban on OT-induced pro-inflammatory responses in amnion cells. Pre-labour amnion epithelial cells were stimulated for 5 min, 15 min, 30 min, 2 h, 4 h and 6 h with Atosiban (10 μM) and/or OT (10 nM). Representative Western blots for phosphorylated NF-κB p65 subunit, ERK1/2 and p38 MAPK (A), as well as COX-2 and p-cPLA$_2$ (B) are shown above their corresponding densitometry graphs with fold changes compared to non-stimulated (NS) controls. Matched β-actin loading controls confirm equal loading (n = 6; * p<0.05, ** p<0.01 compared with NS). Significance was tested using ANOVA, with correction for multiple testing by *Tukey-Kramer* multiple comparison test.

Figure 3. Increase in pro-labour NF-κB-regulated gene expression with Atosiban stimulation in amnion cells. Pre-labour amnion epithelial cells were stimulated for 1 h, 2 h, 4 h, and 6 h with Atosiban (10 μM) and/or OT (10 nM). Expression of downstream NF-κB regulated genes; COX-2 (A), IL-6 (B), CCL5 (C), IL-8 (D) and SOD2 (E) were examined from total RNA extracts. Atosiban had no effect on OT-induced upregulation, but Atosiban alone increased the expression of COX-2, IL-6 and CCL5 (n = 6; * p<0.05, *** p<0.001 compared with NS, ANOVA). Significance was tested using ANOVA, with correction for multiple testing by *Tukey-Kramer* multiple comparison test.

Figure 4. The effect of Nolasiban on OT-mediated activation of NF-κB and MAPKs in amnion cells. Pre-labour primary amnion epithelial cells were stimulated with OT (10 nM) in presence of absence of Nolasiban (1, 3, or 10μM) for 5 min, 15 min and 30 min. Western blots were used to examine the effect of Nolasiban on OT-mediated activation of p65 NF-κB and MAPKs, ERK1/2 and p38 MAPK (A). Solid lines indicated cropping boundaries of strips (please note that this editing is done in the blot

Downloaded from molpharm.aspetjournals.org at ASPET Journals on April 10, 2024

Molecular Pharmacology Fast Forward. Published on February 10, 2017 as DOI: 10.1124/mol.116.106013
This article has not been copyedited and formatted. The final version may differ from this version.

panels in Figs 4A, 9A, 10A). NS controls and OT only treatments were adjusted to contain the vehicle, DMSO, at 0.1% v/v. β-actin confirmed equal protein loading. Densitometric analyses showed significant decreases in OT-mediated activation of p65 (B) and p38 (C) in the presence of Nolasiban, but not ERK1/2 (D). (n=6; * $p<0.05$ vs NS, # $p<0.05$ vs OT-treated samples, ANOVA). Significance was tested using ANOVA, with correction for multiple testing by *Tukey-Kramer* multiple comparison test.

Figure 5. The effect of Nolasiban on OT-mediated expression of PG synthetic enzymes in amnion cells. Pre-labour primary amnion epithelial cells were stimulated with OT (10 nM) in presence of absence of Nolasiban (1, 3, or 10μM) for 2 h, 4 h and 6 h. Western blots were used to examine the effect of Nolasiban on OT-mediated expression of COX-2 and p-cPLA$_2$ (A). NS controls and OT only treatments were adjusted to contain the vehicle, DMSO, at 0.1% v/v. β-actin confirmed equal protein loading. Densitometric analyses showed significant decreases in OT-mediated expression of COX-2 (B) and p-cPLA$_2$ (C) in the presence of Nolasiban (n=6; *** $p<0.001$ vs NS, # $p<0.05$, ## $p<0.01$, ### $p<0.001$ vs OT-treated samples, ANOVA). Significance was tested using ANOVA, with correction for multiple testing by *Tukey-Kramer* multiple comparison test.

Figure 6. The effect of Nolasiban on OT-mediated PGE$_2$ release in amnion cells. Pre-labour primary amnion epithelial cells were stimulated with OT (10 nM) in presence of absence of Nolasiban (1, 3, 10 or 30μM) for 2 h, 4 h and 6 h. PGE$_2$ ELISA demonstrated a significant inhibition of OT-mediated PGE$_2$ production by Nolasiban (n=6; * $p<0.05$, *** $p<0.001$ vs NS, ### $p<0.001$ vs OT-treated samples, ANOVA). Significance was tested using ANOVA, with correction for multiple testing by *Dunn's* multiple comparison test.

Figure 7. The effect of Nolasiban on OT-mediated expression of downstream NF-κB-regulated genes in amnion cells. Pre-labor primary amnion epithelial cells were treated with OT (10 nM) in

Downloaded from molpharm.aspetjournals.org at ASPET Journals on April 10, 2024

Molecular Pharmacology Fast Forward. Published on February 10, 2017 as DOI: 10.1124/mol.116.106013
This article has not been copyedited and formatted. The final version may differ from this version.

presence or absence of Nolasiban (1, 3, 10, or 30μM) for 1 h, 2 h, 4 h, 6 h and 24 h, and changes in the expression of downstream NF-κB-regulated genes, COX-2 (A), IL-8 (B), IL-6 (C), CCL5 (D), CCL2 (E) and SOD2 (F), were analysed using qRT-PCR. For qRT-PCR analysis, target gene mRNA levels were normalised to that of the housekeeping gene, L19 (n=4; * $p<0.05$, *** $p<0.001$ vs NS, # $p<0.05$ vs OT-treated samples, ANOVA). Significance was tested using ANOVA, with correction for multiple testing by *Tukey-Kramer* multiple comparison test.

Figure 8. The effect of Atosiban on OT-induced proinflammatory responses in myometrial cells. Pre-labour myometrial smooth muscle cells were stimulated with OT (10 nM) for 5 min, 15 min, 30 min, 2 h, 4 h and 6 h in presence/absence of Atosiban (10 μM). Representative Western blots for phosphorylated NF-κB p65 subunit, ERK1/2 and p38 MAPK (A), as well as COX-2 and p-cPLA$_2$ (B) shown above their corresponding densitometry graphs with fold changes compared to non-stimulated (NS) controls. Matched β-actin loading controls confirm equal loading (n = 6; * $p<0.05$, ** $p<0.01$, *** $p<0.001$ compared with NS, ANOVA). Significance was tested using ANOVA, with correction for multiple testing by *Tukey-Kramer* multiple comparison test.

Figure 9. The effect of Atosiban on OT-induced upregulation of NF-κB-regulated genes in myometrial cells. Pre-labour myometrial smooth muscle cells were stimulated for 1 h, 2 h, 4 h, and 6 h with Atosiban (10 μM) and/or OT (10 nM). Expression of downstream NF-κB regulated genes; COX-2 (A), IL-6 (B), CCL5 (C), IL-8 (D) and SOD2 (E) were examined from total RNA extracts. Atosiban inhibited the effect on OT-induced upregulation of COX-2, IL-6, and IL-8, but Atosiban failed to inhibit CCL5 expression and it alone increased the expression of CCL5 (n = 6; * $p<0.05$ vs NS, # $p<0.05$ vs OT-treated samples, ANOVA). Significance was tested using ANOVA, with correction for multiple testing by *Tukey-Kramer* multiple comparison test.

Downloaded from molpharm.aspetjournals.org at ASPET Journals on April 10, 2024

Molecular Pharmacology Fast Forward. Published on February 10, 2017 as DOI: 10.1124/mol.116.106013
This article has not been copyedited and formatted. The final version may differ from this version.

Figure 10. The effect of Nolasiban on OT-mediated activation of NF-κB and MAPKs in myometrial cells. Pre-labour primary myometrial smooth muscle cells were stimulated with OT (10 nM) in presence of absence of Nolasiban (1, 3, or 10μM) for 5 min, 15 min and 30 min. Western blots were used to examine the effect of Nolasiban on OT-mediated activation of p65 NF-κB and MAPKs, ERK and p38 (A). NS controls and OT only treatments were adjusted to contain the vehicle, DMSO, at 0.1% v/v. β-actin confirmed equal protein loading. Densitometric analyses showed significant decreases in OT-mediated activation of p65 (B) and p38 (C) in the presence of Nolasiban, but not ERK1/2 (D). (n=6; * p<0.05, ** p<0.01; *** p<0.001 vs NS, ## p<0.01 vs OT-treated samples, ANOVA). Significance was tested using ANOVA, with correction for multiple testing by *Tukey-Kramer* multiple comparison test.

Figure 11. The effect of Nolasiban on OT-mediated expression of PG synthetic enzymes in myometrial cells. Pre-labour primary myometrial smooth muscle cells were stimulated with OT (10 nM) in presence of absence of Nolasiban (1, 3, or 10μM) for 2 h, 4 h and 6 h. Western blots to examine the effect of Nolasiban on OT-mediated expression of COX-2 and p-cPLA$_2$ (A). NS controls and OT only treatments were adjusted to contain the vehicle, DMSO, at 0.1% v/v. β-actin confirmed equal protein loading. Densitometric analyses showed significant decreases in OT-mediated expression of COX-2 (B) and p-cPLA$_2$ (C) in the presence of Nolasiban (n=6; ** p<0.01, *** p<0.001 vs NS, ## p<0.01, ### p<0.001 vs OT-treated samples, ANOVA). Significance was tested using ANOVA, with correction for multiple testing by *Tukey-Kramer* multiple comparison test.

Figure 12. The effect of Nolasiban on OT-mediated PGE$_2$ release in myometrial cells. Pre-labour primary myometrial smooth muscle cells were stimulated with OT (10 nM) in presence of absence of Nolasiban (1, 3, 10 or 30μM) for 2 h, 4 h and 6 h. PGE$_2$ ELISA demonstrated a significant inhibition of OT-mediated PGE$_2$ production by Nolasiban (n=6; ** p<0.01, *** p<0.001 vs NS, ## p<0.01, ###

Downloaded from molpharm.aspetjournals.org at ASPET Journals on April 10, 2024

Molecular Pharmacology Fast Forward. Published on February 10, 2017 as DOI: 10.1124/mol.116.106013
This article has not been copyedited and formatted. The final version may differ from this version.

p<0.001 vs OT-treated samples, ANOVA). Significance was tested using ANOVA, with correction for multiple testing by *Dunn's* multiple comparison test.

Figure 13. The effect of Nolasiban on OT-mediated expression of downstream NF-κB-regulated genes in myometrial cells. Pre-labour primary myometrial smooth muscle cells were treated with OT (10 nM) in presence or absence of Nolasiban (1, 3, 10, or 30μM) for 1 h, 2 h, 4 h, 6 h and 24 h, and the expression of downstream NF-κB-regulated genes, COX-2 (A), IL-8 (B), IL-6 (C), CCL5 (D), CCL2 (E) and SOD2 (F) were analysed using qRT-PCR. For qRT-PCR analysis, target gene mRNA levels were normalised to that of the housekeeping gene, GAPDH (n=4; * *p*<0.05, *** *p*<0.001 vs NS, # *p*<0.05 vs OT-treated samples, ANOVA). Significance was tested using ANOVA, with correction for multiple testing by *Tukey-Kramer* multiple comparison test.

Figure 14. Schematic diagram describing the effects of OT, Atosiban and Nolasiban on downstream signaling pathways in both human amnion and myometrium. Our data indicate that in amnion, Atosiban mimics the proinflammatory effects of OT whereas Nolasiban completely inhibits the effects of OT. In myometrium, Atosiban appears to show biased agonist properties where it acts as an antagonist to inhibit myometrial contractions whilst driving expression of NF-κB-regulated gene, CCL5. Similar to amnion, Nolasiban appeared to inhibit both the inflammatory and contractile effects of OT.

Downloaded from molpharm.aspetjournals.org at ASPET Journals on April 10, 2024

Molecular Pharmacology Fast Forward. Published on February 10, 2017 as DOI: 10.1124/mol.116.106013
This article has not been copyedited and formatted. The final version may differ from this version.

Table 1. Primer sequences for real-time PCR (RT-PCR)

Target Gene	Forward Primer Sequence (5' to 3')	Reverse Primer Sequence (5' to 3')
L19	GCGGAAGGGTACAGCCAAT	GCAGCCGGCGCAAA
GAPDH	TGATGACATCAAGAAGGTGGTGAAG	TCCTTGGAGGCCATGTAGGCCAT
CCL2	TCTGTGCCTGCTGCTCATAG	AGATCTCCTTGGCCACAATG
CCL5	CCATATTCCTCGGACACCAC	TGTACTCCCGAACCCATTTC
COX-2	TGTGCAACACTTGAGTGGCT	ACTTTCTGTACTGCGGGTGG
IL-6	CCTTCCAAAGATGGCTGAAA	AGCTCTGGCTTGTTCCTCAC
IL-8	GCCTTCCTGATTTCTGCAGC	CGCAGTGTGGTCCACTCTCA
SOD2	TTGGCCAAGGGAGATGTTAC	AGTCACGTTTGATGGCTTCC

Downloaded from molpharm.aspetjournals.org at ASPET Journals on April 10, 2024

Figure 1

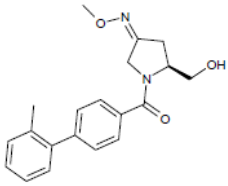

Figure 2

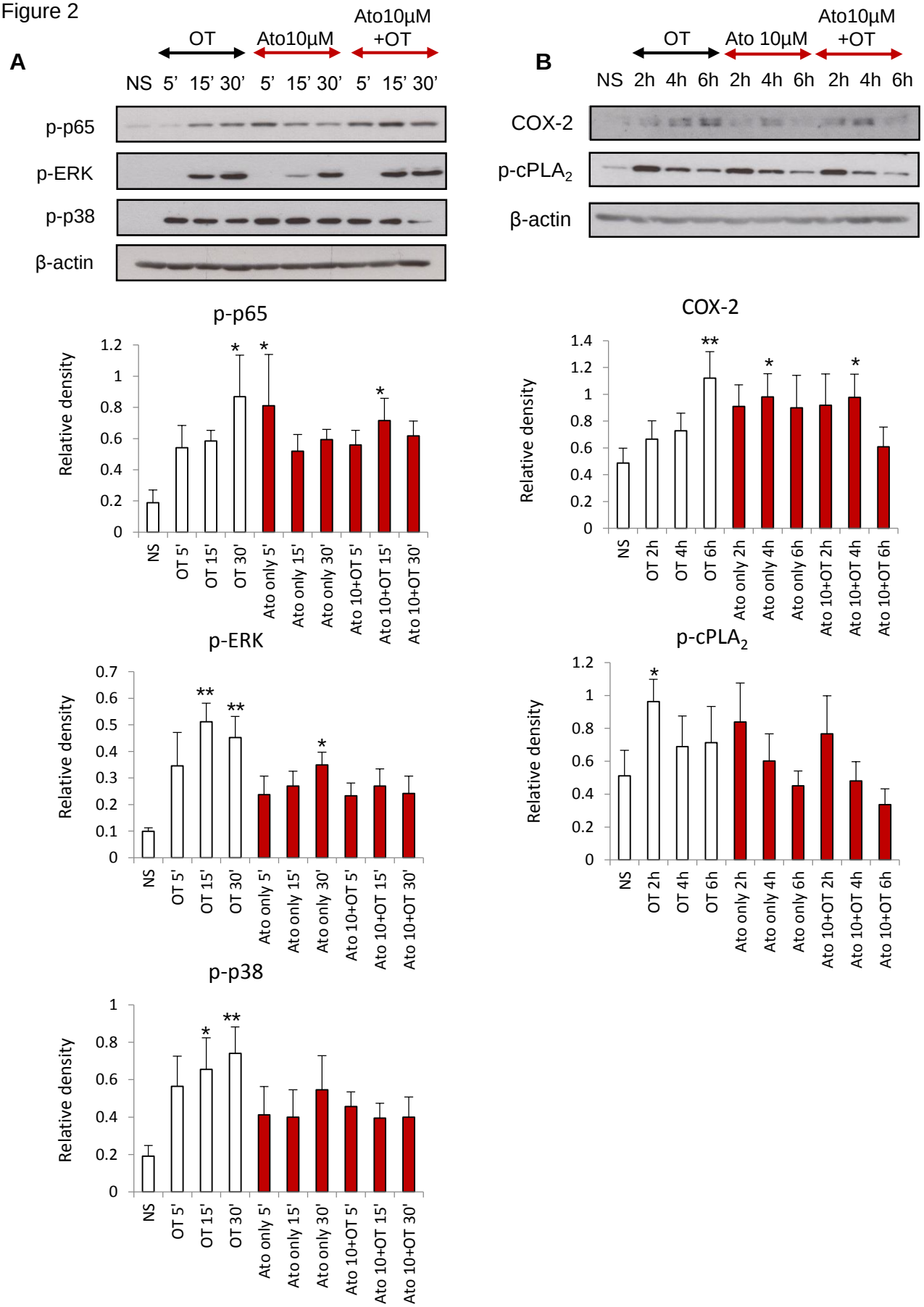
A
OT
Ato10μM
Ato10μM +OT
NS 5' 15' 30' 5' 15' 30' 5' 15' 30'
p-p65
p-ERK
p-p38
β-actin
B
OT
Ato 10μM
Ato10μM +OT
NS 2h 4h 6h 2h 4h 6h 2h 4h 6h
COX-2
p-cPLA2
β-actin
p-p65
Relative density
NS
OT 5'
OT 15'
OT 30'
Ato only 5'
Ato only 15'
Ato only 30'
Ato 10+OT 5'
Ato 10+OT 15'
Ato 10+OT 30'
COX-2
OT 2h
OT 4h
OT 6h
Ato only 2h
Ato only 4h
Ato only 6h
Ato 10+OT 2h
Ato 10+OT 4h
Ato 10+OT 6h
p-ERK
p-cPLA2
p-p38

Figure 3

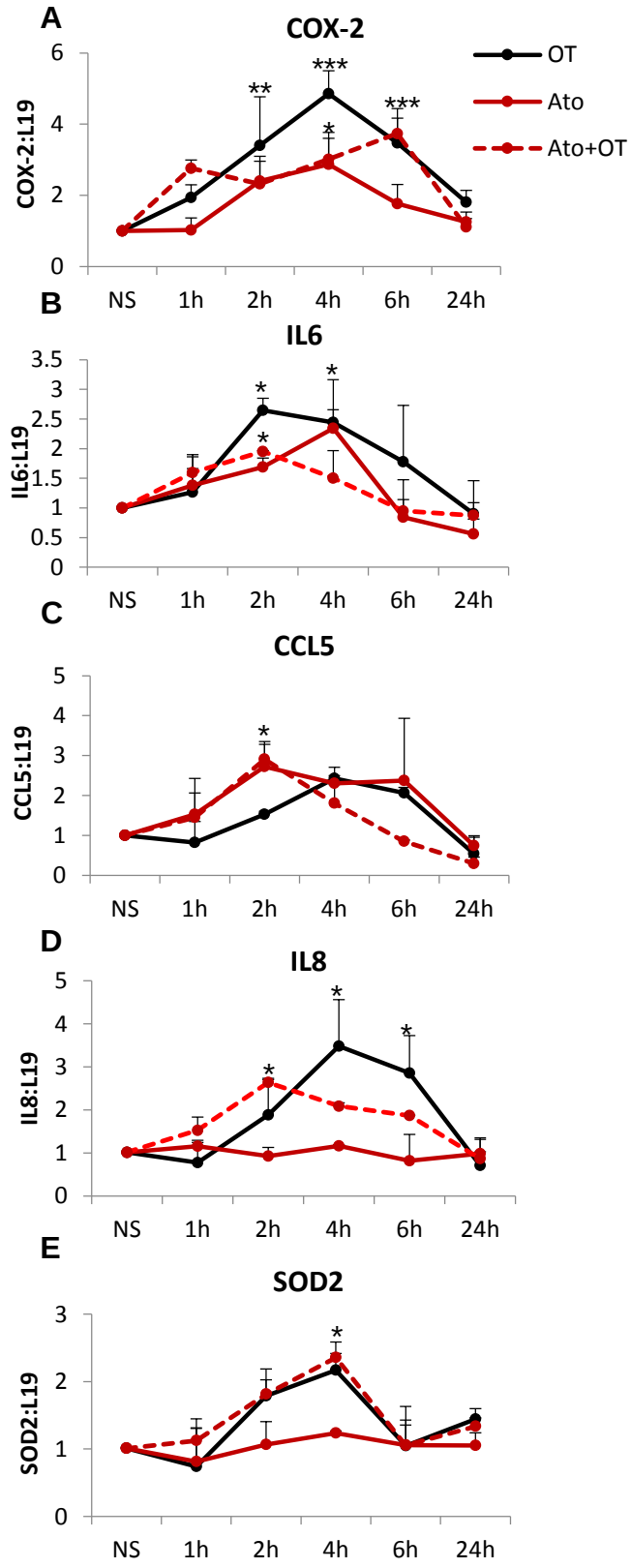
A
COX-2
COX-2:L19
OT
Ato
Ato+OT
NS
1h
2h
4h
6h
24h
B
IL6
IL6:L19
C
CCL5
CCL5:L19
D
IL8
IL8:L19
E
SOD2
SOD2:L19

Figure 4

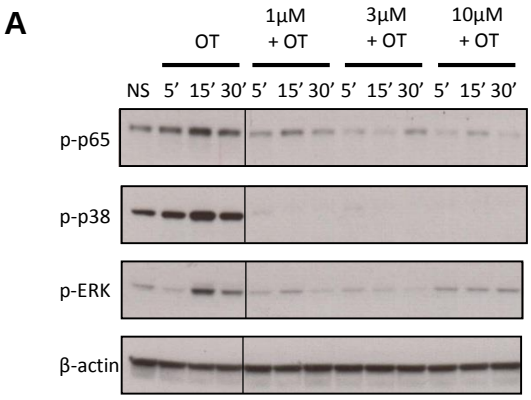
A
OT
1μM + OT
3μM + OT
10μM + OT
NS 5′ 15′ 30′ 5′ 15′ 30′ 5′ 15′ 30′ 5′ 15′ 30′
p-p65
p-p38
p-ERK
β-actin

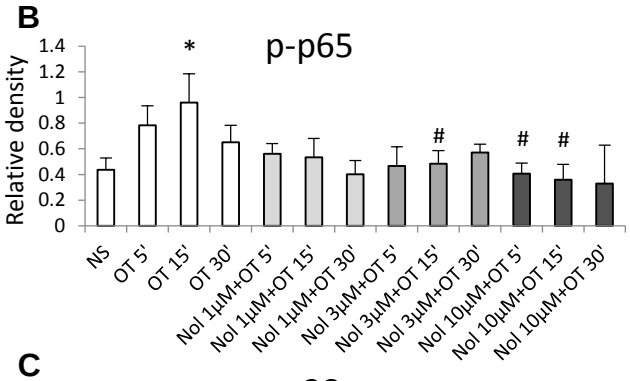
B
p-p65
Relative density
1.4
1.2
1
0.8
0.6
0.4
0.2
0
NS
OT 5'
OT 15'
OT 30'
Nol 1μM+OT 5'
Nol 1μM+OT 15'
Nol 1μM+OT 30'
Nol 3μM+OT 5'
Nol 3μM+OT 15'
Nol 3μM+OT 30'
Nol 10μM+OT 5'
Nol 10μM+OT 15'
Nol 10μM+OT 30'

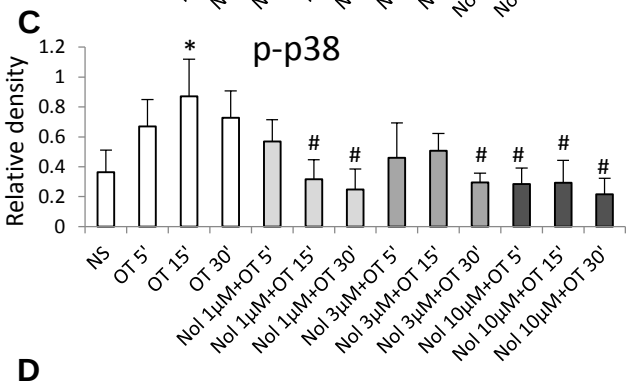
C
p-p38
Relative density
1.2
1
0.8
0.6
0.4
0.2
0
NS
OT 5'
OT 15'
OT 30'
Nol 1μM+OT 5'
Nol 1μM+OT 15'
Nol 1μM+OT 30'
Nol 3μM+OT 5'
Nol 3μM+OT 15'
Nol 3μM+OT 30'
Nol 10μM+OT 5'
Nol 10μM+OT 15'
Nol 10μM+OT 30'

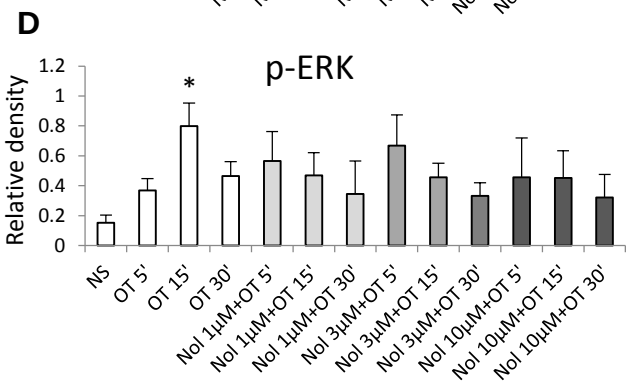
D
p-ERK
Relative density
1.2
1
0.8
0.6
0.4
0.2
0
NS
OT 5'
OT 15'
OT 30'
Nol 1μM+OT 5'
Nol 1μM+OT 15'
Nol 1μM+OT 30'
Nol 3μM+OT 5'
Nol 3μM+OT 15'
Nol 3μM+OT 30'
Nol 10μM+OT 5'
Nol 10μM+OT 15'
Nol 10μM+OT 30'

Figure 5

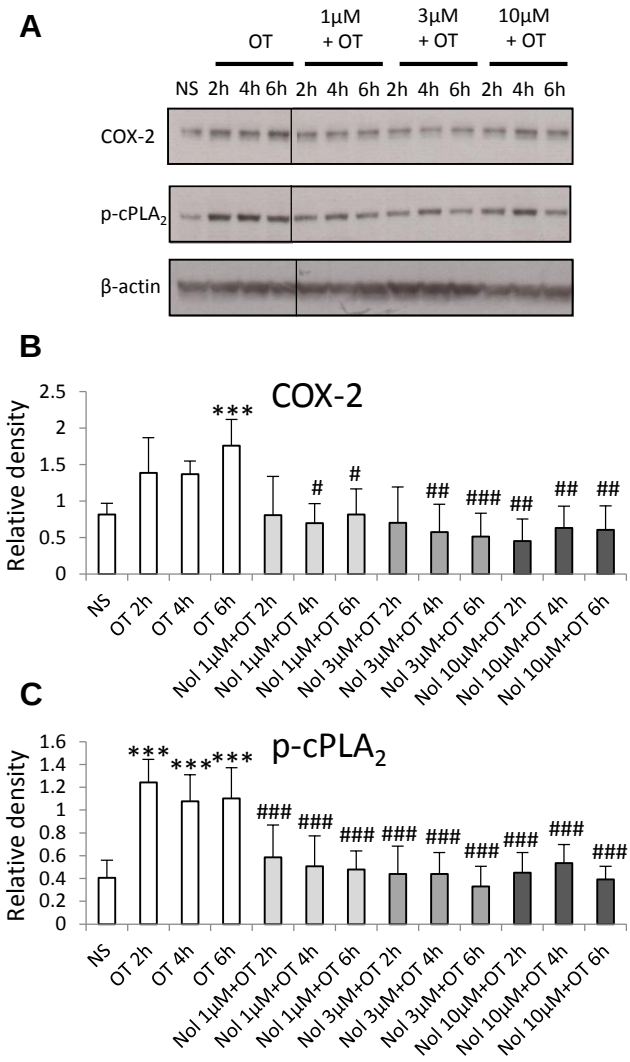
A
OT
1μM + OT
3μM + OT
10μM + OT
NS 2h 4h 6h 2h 4h 6h 2h 4h 6h 2h 4h 6h
COX-2
p-cPLA2
β-actin
B
COX-2
Relative density
2.5
2
1.5
1
0.5
0
***
#
#
##
###
##
##
##
NS
OT 2h
OT 4h
OT 6h
Nol 1μM+OT 2h
Nol 1μM+OT 4h
Nol 1μM+OT 6h
Nol 3μM+OT 2h
Nol 3μM+OT 4h
Nol 3μM+OT 6h
Nol 10μM+OT 2h
Nol 10μM+OT 4h
Nol 10μM+OT 6h
C
p-cPLA2
Relative density
1.6
1.4
1.2
1
0.8
0.6
0.4
0.2
0
***
***
***
###
###
###
###
###
###
###
###
###
NS
OT 2h
OT 4h
OT 6h
Nol 1μM+OT 2h
Nol 1μM+OT 4h
Nol 1μM+OT 6h
Nol 3μM+OT 2h
Nol 3μM+OT 4h
Nol 3μM+OT 6h
Nol 10μM+OT 2h
Nol 10μM+OT 4h
Nol 10μM+OT 6h

Figure 6

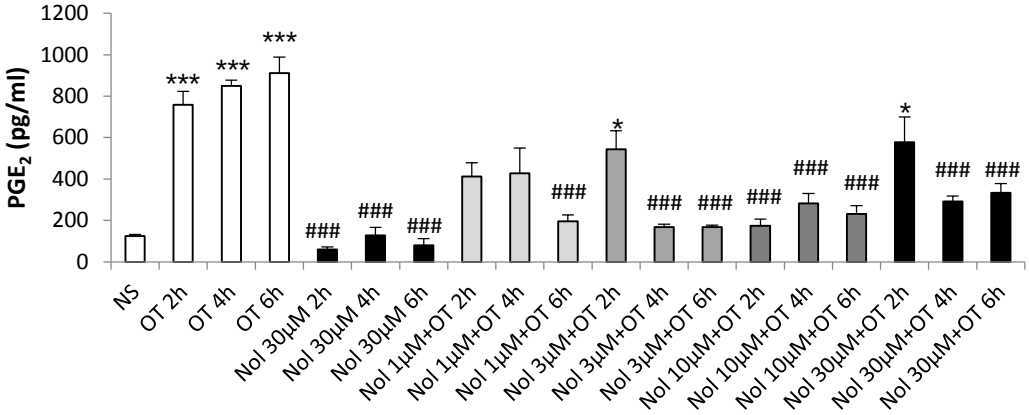
PGE2 (pg/ml)
1200
1000
800
600
400
200
0
***
***
***
###
###
###
###
###
*
###
###
###
###
###
*
###
###
NS
OT 2h
OT 4h
OT 6h
Nol 30µM 2h
Nol 30µM 4h
Nol 30µM 6h
Nol 1µM+OT 2h
Nol 1µM+OT 4h
Nol 1µM+OT 6h
Nol 3µM+OT 2h
Nol 3µM+OT 4h
Nol 3µM+OT 6h
Nol 10µM+OT 2h
Nol 10µM+OT 4h
Nol 10µM+OT 6h
Nol 30µM+OT 2h
Nol 30µM+OT 4h
Nol 30µM+OT 6h

Figure 7

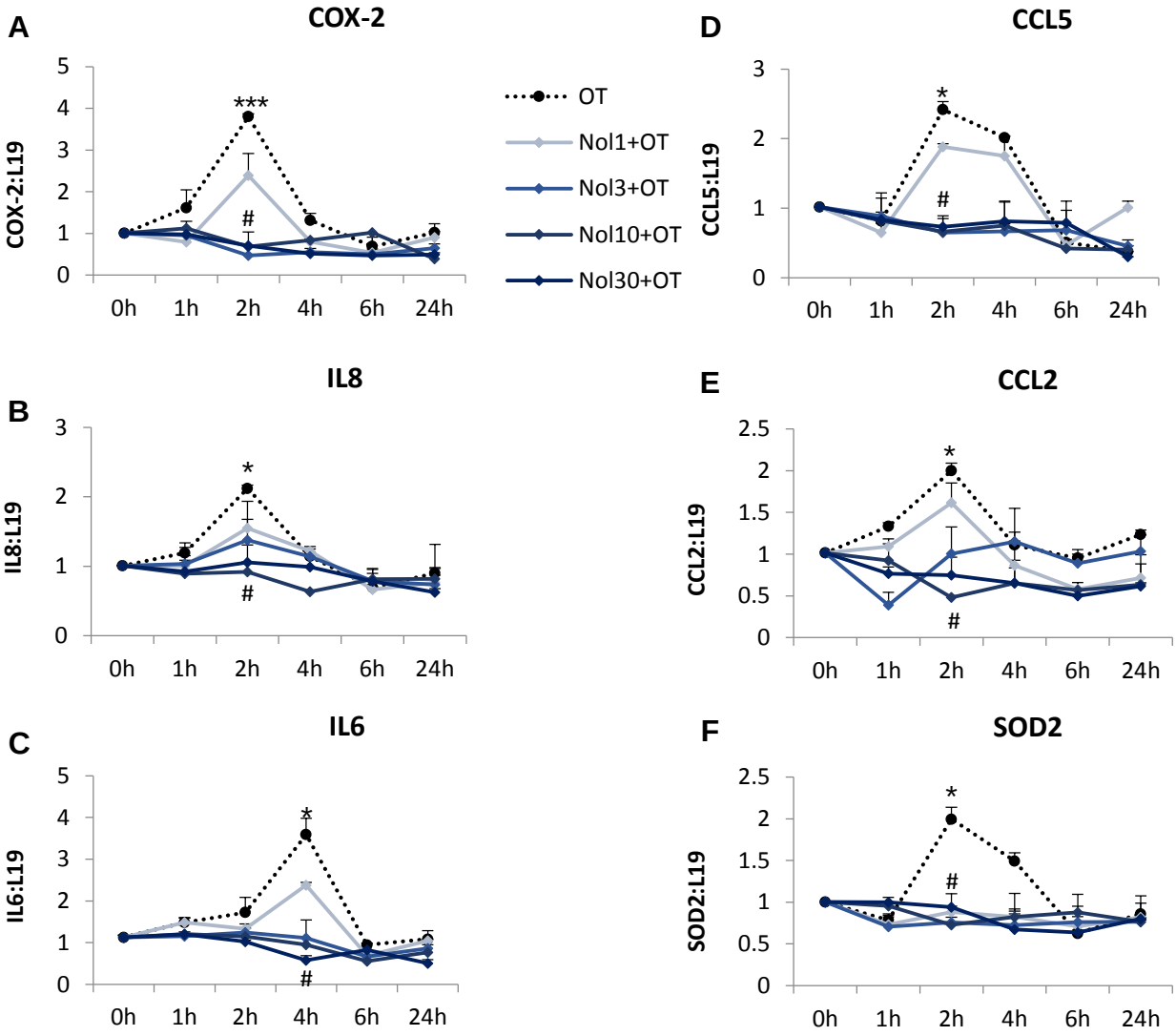
A
COX-2
COX-2:L19
***
#
0h 1h 2h 4h 6h 24h
OT
Nol1+OT
Nol3+OT
Nol10+OT
Nol30+OT
D
CCL5
CCL5:L19
*
#
B
IL8
IL8:L19
*
#
E
CCL2
CCL2:L19
*
#
C
IL6
IL6:L19
*
#
F
SOD2
SOD2:L19
*
#

Figure 8

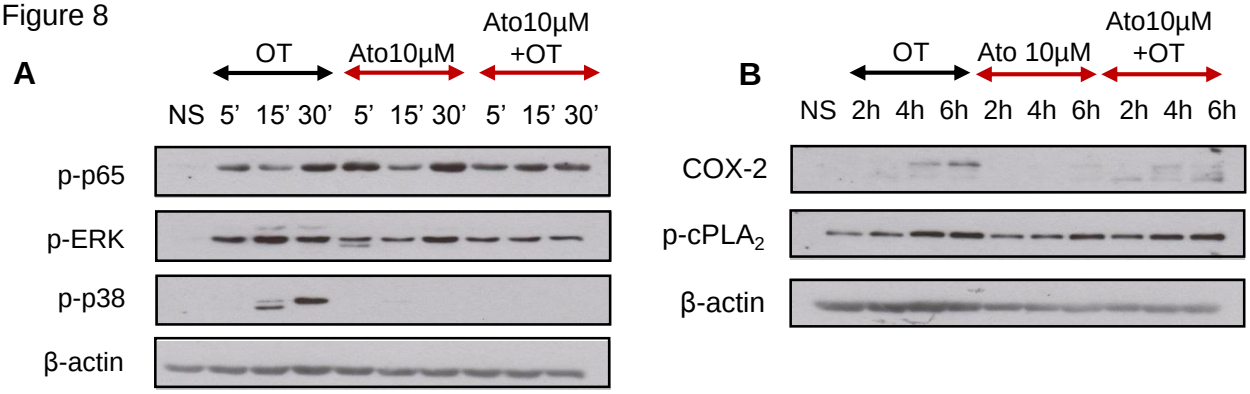
A
OT
Ato10μM
Ato10μM +OT
NS 5' 15' 30' 5' 15' 30' 5' 15' 30'
p-p65
p-ERK
p-p38
β-actin
B
OT
Ato 10μM
Ato10μM +OT
NS 2h 4h 6h 2h 4h 6h 2h 4h 6h
COX-2
p-cPLA2
β-actin

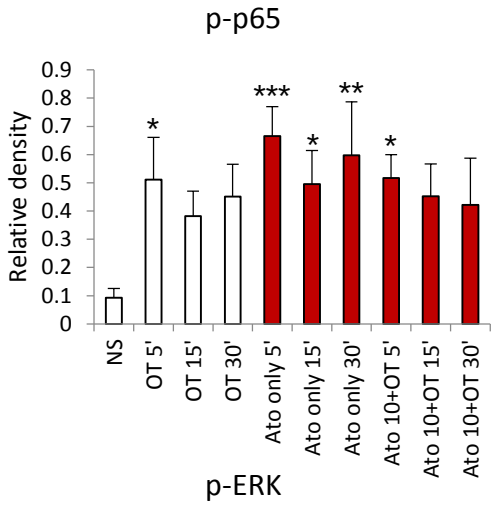
p-p65
Relative density
NS
OT 5'
OT 15'
OT 30'
Ato only 5'
Ato only 15'
Ato only 30'
Ato 10+OT 5'
Ato 10+OT 15'
Ato 10+OT 30'

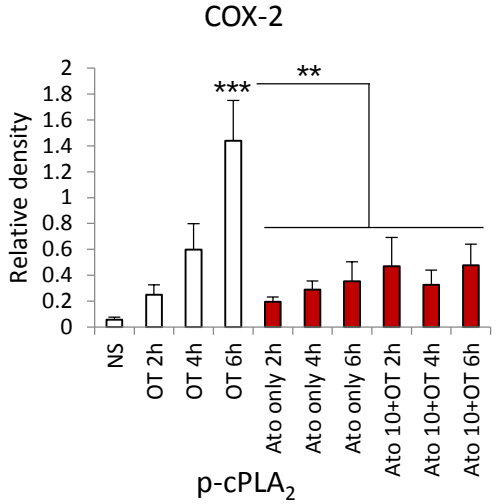
COX-2
Relative density
NS
OT 2h
OT 4h
OT 6h
Ato only 2h
Ato only 4h
Ato only 6h
Ato 10+OT 2h
Ato 10+OT 4h
Ato 10+OT 6h

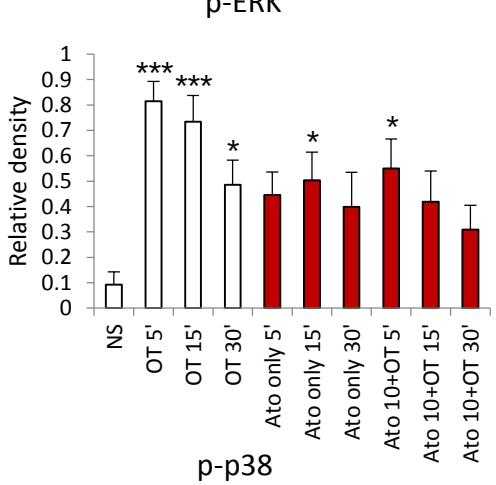
p-ERK
Relative density
NS
OT 5'
OT 15'
OT 30'
Ato only 5'
Ato only 15'
Ato only 30'
Ato 10+OT 5'
Ato 10+OT 15'
Ato 10+OT 30'

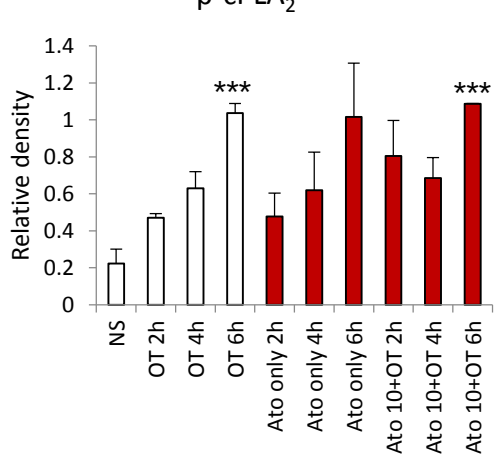
p-cPLA2
Relative density
NS
OT 2h
OT 4h
OT 6h
Ato only 2h
Ato only 4h
Ato only 6h
Ato 10+OT 2h
Ato 10+OT 4h
Ato 10+OT 6h

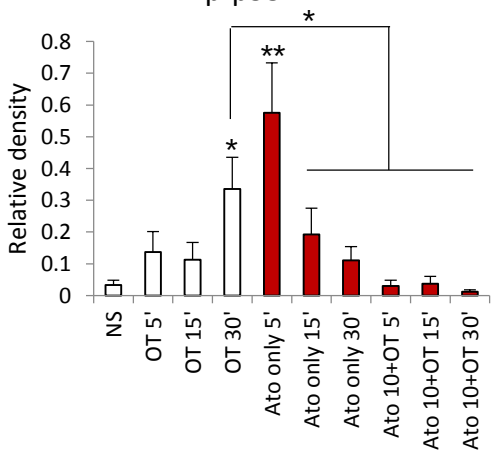
p-p38
Relative density
NS
OT 5'
OT 15'
OT 30'
Ato only 5'
Ato only 15'
Ato only 30'
Ato 10+OT 5'
Ato 10+OT 15'
Ato 10+OT 30'

Figure 9

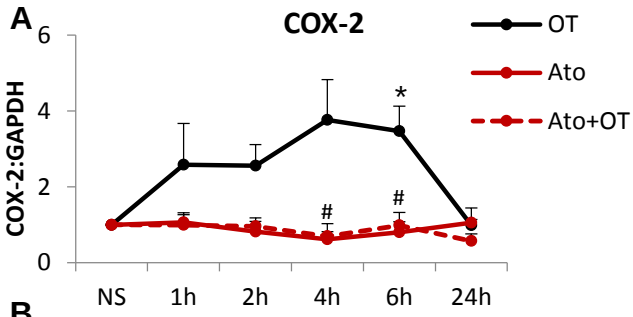
A
COX-2
OT
Ato
Ato+OT
COX-2:GAPDH
0
2
4
6
*
#
#
NS
1h
2h
4h
6h
24h

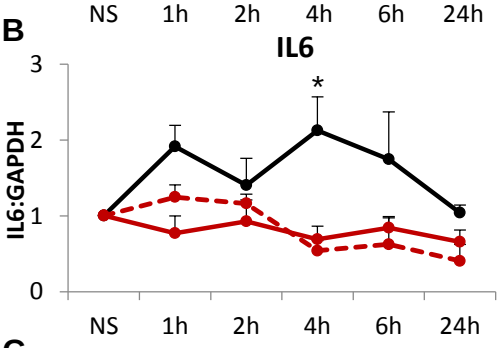
B
IL6
IL6:GAPDH
0
1
2
3
*
NS
1h
2h
4h
6h
24h

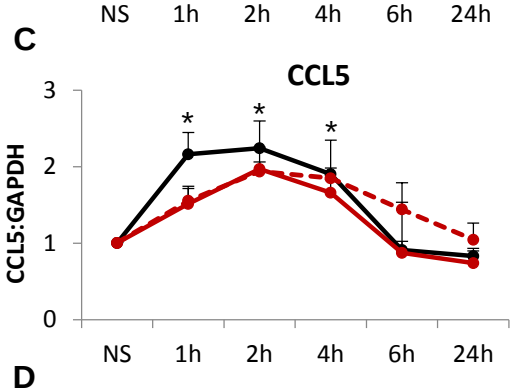
C
CCL5
CCL5:GAPDH
0
1
2
3
*
*
*
NS
1h
2h
4h
6h
24h

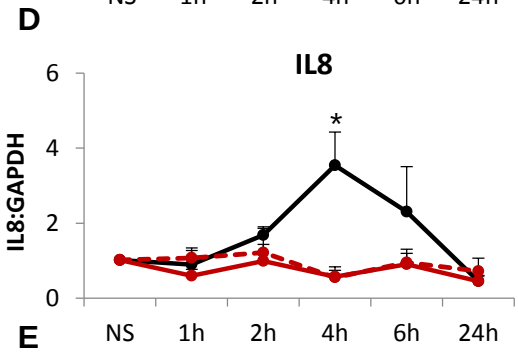
D
IL8
IL8:GAPDH
0
2
4
6
*
NS
1h
2h
4h
6h
24h

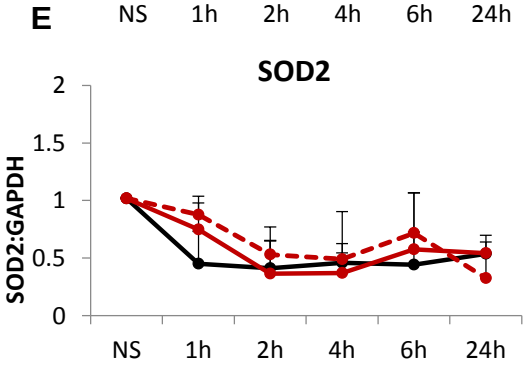
E
SOD2
SOD2:GAPDH
0
0.5
1
1.5
2
NS
1h
2h
4h
6h
24h

Figure 10

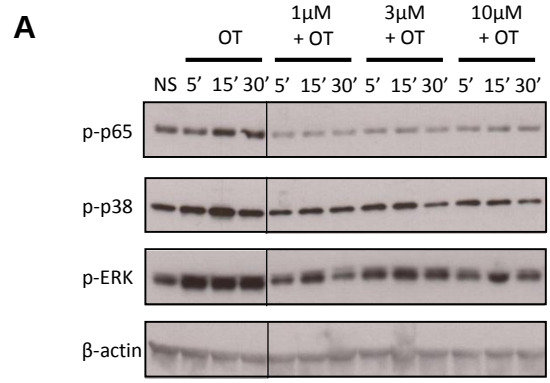
A
OT
1μM + OT
3μM + OT
10μM + OT
NS 5′ 15′ 30′ 5′ 15′ 30′ 5′ 15′ 30′ 5′ 15′ 30′
p-p65
p-p38
p-ERK
β-actin

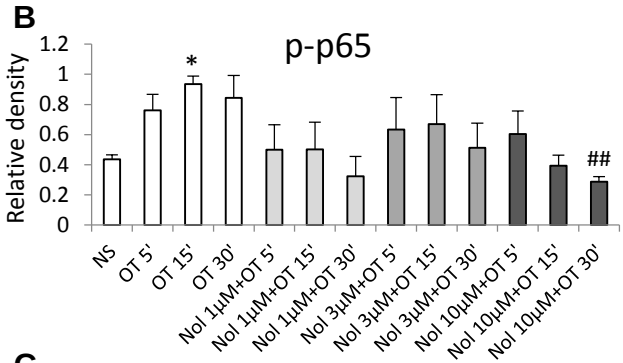
B
p-p65
Relative density
1.2
1
0.8
0.6
0.4
0.2
0
*
##
NS
OT 5'
OT 15'
OT 30'
Nol 1μM+OT 5'
Nol 1μM+OT 15'
Nol 1μM+OT 30'
Nol 3μM+OT 5'
Nol 3μM+OT 15'
Nol 3μM+OT 30'
Nol 10μM+OT 5'
Nol 10μM+OT 15'
Nol 10μM+OT 30'

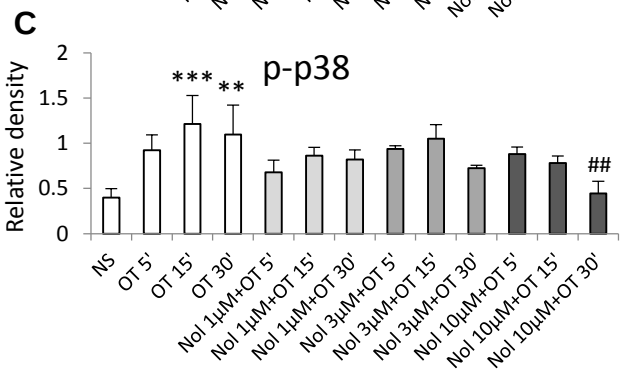
C
p-p38
Relative density
2
1.5
1
0.5
0
***
**
##
NS
OT 5'
OT 15'
OT 30'
Nol 1μM+OT 5'
Nol 1μM+OT 15'
Nol 1μM+OT 30'
Nol 3μM+OT 5'
Nol 3μM+OT 15'
Nol 3μM+OT 30'
Nol 10μM+OT 5'
Nol 10μM+OT 15'
Nol 10μM+OT 30'

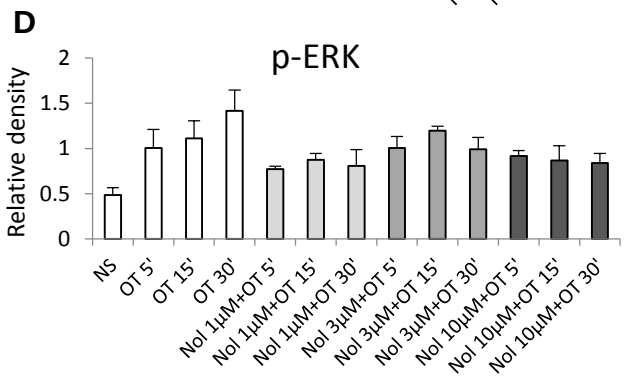
D
p-ERK
Relative density
2
1.5
1
0.5
0
NS
OT 5'
OT 15'
OT 30'
Nol 1μM+OT 5'
Nol 1μM+OT 15'
Nol 1μM+OT 30'
Nol 3μM+OT 5'
Nol 3μM+OT 15'
Nol 3μM+OT 30'
Nol 10μM+OT 5'
Nol 10μM+OT 15'
Nol 10μM+OT 30'

Figure 11

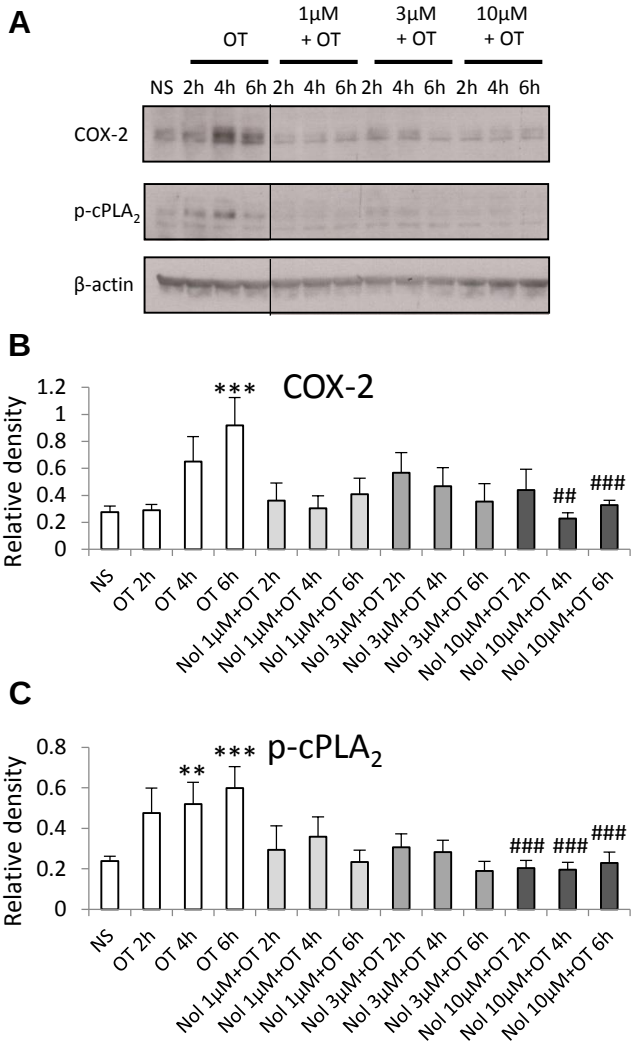
A
OT
1μM + OT
3μM + OT
10μM + OT
NS 2h 4h 6h 2h 4h 6h 2h 4h 6h 2h 4h 6h
COX-2
p-cPLA2
β-actin
B
COX-2
Relative density
1.2
1
0.8
0.6
0.4
0.2
0
***
##
###
NS
OT 2h
OT 4h
OT 6h
Nol 1μM+OT 2h
Nol 1μM+OT 4h
Nol 1μM+OT 6h
Nol 3μM+OT 2h
Nol 3μM+OT 4h
Nol 3μM+OT 6h
Nol 10μM+OT 2h
Nol 10μM+OT 4h
Nol 10μM+OT 6h
C
p-cPLA2
Relative density
0.8
0.6
0.4
0.2
0
**
***
###
###
###
NS
OT 2h
OT 4h
OT 6h
Nol 1μM+OT 2h
Nol 1μM+OT 4h
Nol 1μM+OT 6h
Nol 3μM+OT 2h
Nol 3μM+OT 4h
Nol 3μM+OT 6h
Nol 10μM+OT 2h
Nol 10μM+OT 4h
Nol 10μM+OT 6h

Figure 12

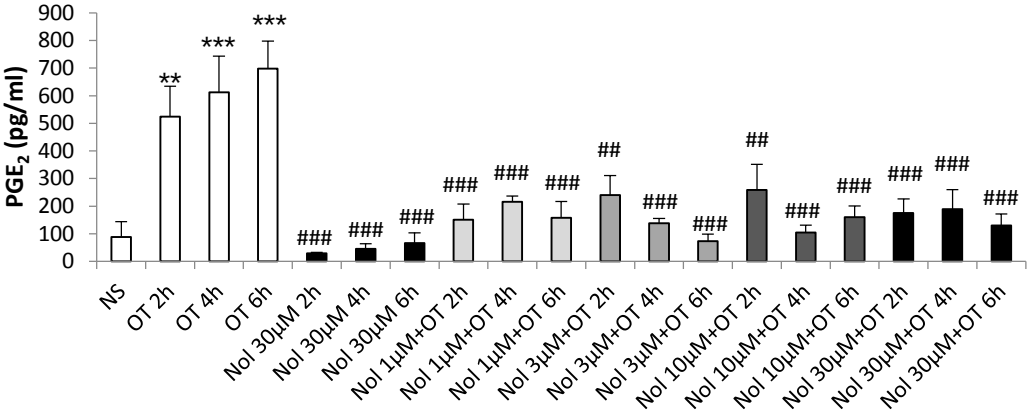
PGE2 (pg/ml)
900
800
700
600
500
400
300
200
100
0
NS
OT 2h
OT 4h
OT 6h
Nol 30µM 2h
Nol 30µM 4h
Nol 30µM 6h
Nol 1µM+OT 2h
Nol 1µM+OT 4h
Nol 1µM+OT 6h
Nol 3µM+OT 2h
Nol 3µM+OT 4h
Nol 3µM+OT 6h
Nol 10µM+OT 2h
Nol 10µM+OT 4h
Nol 10µM+OT 6h
Nol 30µM+OT 2h
Nol 30µM+OT 4h
Nol 30µM+OT 6h
**
***
***
###
###
###
###
###
###
##
###
###
##
###
###
###
###
###

Figure 13

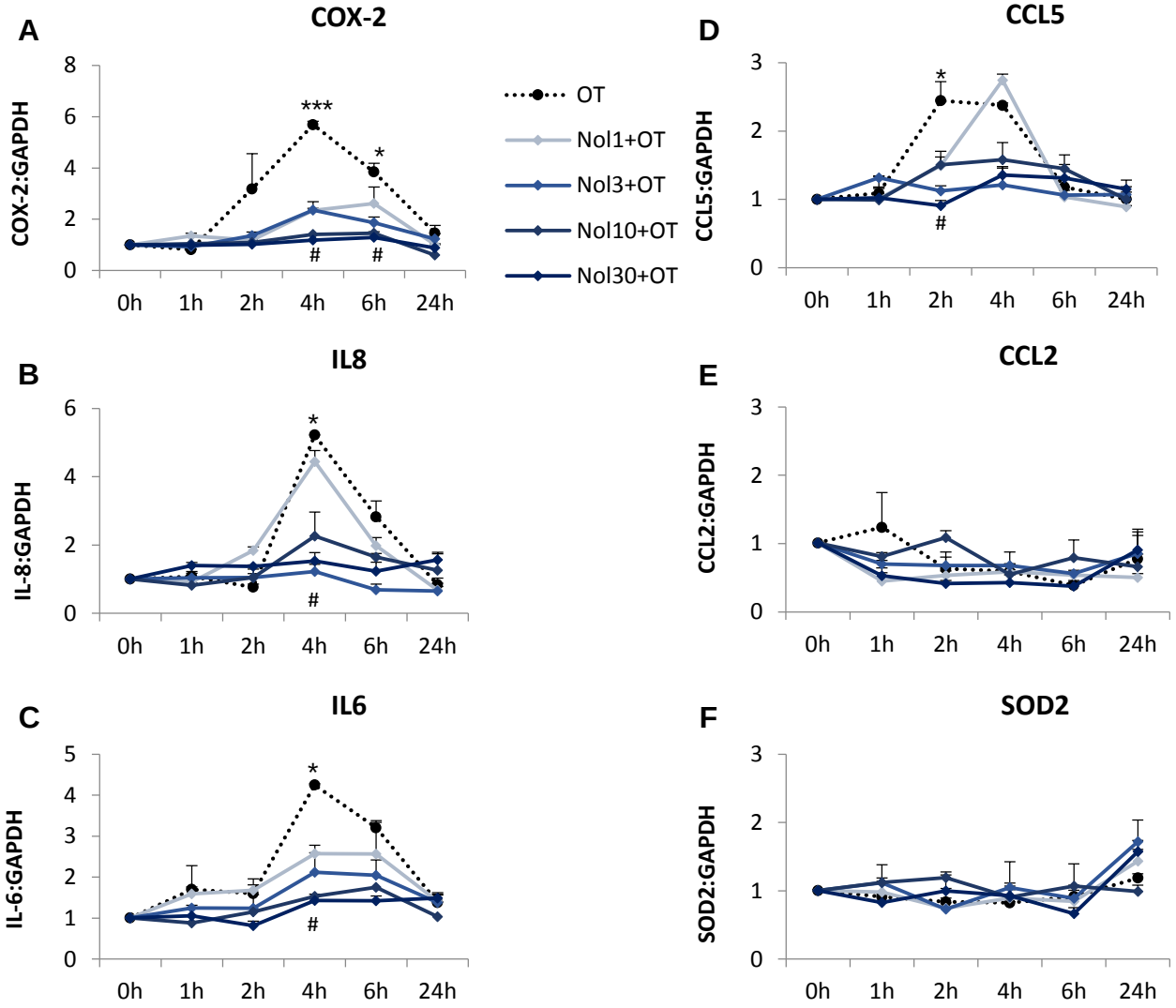
A
COX-2
COX-2:GAPDH
OT
Nol1+OT
Nol3+OT
Nol10+OT
Nol30+OT
0h
1h
2h
4h
6h
24h
B
IL8
IL-8:GAPDH
C
IL6
IL-6:GAPDH
D
CCL5
CCL5:GAPDH
E
CCL2
CCL2:GAPDH
F
SOD2
SOD2:GAPDH

Figure 14

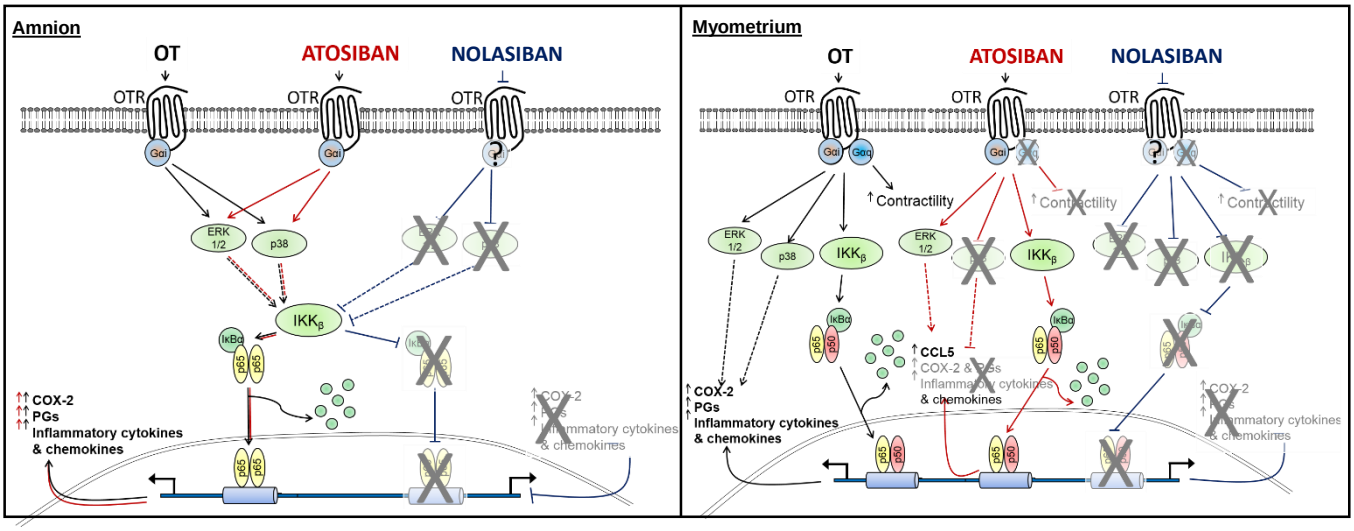
Amnion
OT
ATOSIBAN
NOLASIBAN
OTR
Gαi
ERK 1/2
p38
IKKβ
IκBα
p65
p50
↑↑ COX-2
↑↑ PGs
Inflammatory cytokines & chemokines
Myometrium
↑ Contractility
↑ CCL5
↑ COX-2 & PGs
↑ COX-2
↑ PGs
Inflammatory cytokines & chemokines